AUT Journal of Mechanical Engineering

AUT J. Mech. Eng., 6(3) (2022) 315-330
DOI: 10.22060/ajme.2022.20897.6023

Development of Theoretical Model to calculate Steam Hammer Force on Shock Absorber in Multi Series Pipeline

H. Nouri*

Department of Mechanical Engineering, Sanandaj Branch, Islamic Azad University, Sanandaj, Iran

ABSTRACT: This research work allocates to physical models in order to simulate real world results of the steam hammer at turbine multi-series pipeline in power plants. The aim of this study is to investigate the effect of a steam hammer on a steam turbine line and calculation the force on the shock absorber at the end of the main pipeline. For this purpose, the new theoretical model based on thermodynamic relationships and accurate calculation of wave speed propagation was developed and implemented into the physical model. The main achievement of this research is to present a simple and accurate theoretical model that can provide a bridge between hydro-mechanical data and estimates the impact force of the steam hammer on piping with less computational effort than finite element and a less costly setup than experimental models. The method of characteristics as a complement to the theoretical model was applied and compared. In this work, special attention is devoted to the study of the most relevant process parameters, with emphasis on their meaning, effects, and mutual interaction. The present paper organizes a theoretical model and numerical method of characteristics to predict steam hammer transients behavior in a multi-series pipeline. The initial results are promising and indicate the possibility of using the proposed simple yet, but efficient theoretical model than finite element models in terms of quality, cost, and time consumption of producing results.

Review History:

Received: Dec. 18, 2021
Revised: Apr. 19, 2022
Accepted: Apr. 28, 2022
Available Online: May, 05, 2022

Keywords:

Steam hammer
Multi series pipeline
Theoretical modeling
Method of characteristics
Shock absorber

1- Introduction

The first research on the interaction mechanism between transient flow and pipe wall resistance considering fluid compressibility was done in the 19th century by Korteweg and Helmholtz [1, 2] and then other researchers based on the same principles developed their knowledge in the field of steam hammer [3]. Large long pipes nowadays in the modern world are widely used to transfer fluids, especially in power plants. High pressure and flow due to the rapid closing of the control valve and consequent steam hammer affect the fluid flow inside these pipes. The force caused by the impact of the steam hammer damages the piping if exceeds the bearing threshold of pipe walls. Therefore, understanding the mechanism of the steam hammer and calculating the force caused by the steam hammer is a necessity. Steam hammer is a term that refers to the transient pressure peaks which occur in a pipe when there is a rapid change in the flow velocity within it. Fig. l illustrates how a velocity change caused by an instantaneous closure of a gate at the end of a pipe creates pressure waves traveling within the pipe. Initially, steam flows at some velocity v_0 as shown in (a). When the gate is closed, the steam flowing within the pipe has a tendency to continue flowing because of its momentum. Because it is physically prevented from so doing, it piles up behind the gate; the kinetic energy of the element of steam nearest the gate is converted to pressure energy, which slightly compresses the steam and expands the circumference of the pipe at this point (b). This action is repeated by the following elements of steam (c), and the wavefront of increased pressure travels the length of the pipe until the velocity of the steam v_0 is destroyed, the steam is compressed, and the pipe is expanded its entire length (d). At this point, the steam's kinetic energy has all been converted to strain energy of the steam (under increased compression) and strain energy of the pipe (under increased tension). Because the steam in the reservoir remains under normal static pressure but the steam in the pipe is now under higher pressure, the flow reverses and is forced back into the reservoir again with velocity v_0 (e). As the steam under compression starts flowing back, the pressure in the pipe is reduced to normal static pressure. A pressure unloading wave then travels down the pipe toward the gate (f) until all the strain energy is converted back into kinetic energy (g). However, unlike case (a), the steam is now flowing in the opposite direction and because of its momentum, the steam again tries to maintain this velocity. In so doing, it stretches the element of steam nearest the gate, reducing the pressure there and contracting the pipe (h). This happens with successive elements of steam and a

*Corresponding author's email: Hnouri@iausdj.ac.ir

negative pressure wave propagates back to the reservoir (i) until the entire pipe is under compression and steam under reduced pressure (j). This negative pressure wave would have the same absolute magnitude as the initial positive pressure wave if it is assumed that friction losses do not exist. The velocity then returns to zero but the lower pressure in the pipe compared to that in the reservoir forces steam to flow back into the pipe (k). The pressure surge travels back toward the gate (e) until the entire cycle is complete and a second cycle commences (b). The velocity with which the pressure front moves is a function of the speed of sound in steam modified by the elastic characteristics of the pipe material. In reality, the penstock pipe is usually inclined but the effect remains the same, with the surge pressure at each point along the pipe adding to or subtracting from the static pressure at that point. In addition, the damping effect of friction within the pipe causes the kinetic energy of the flow to dissipate gradually and the amplitude of the pressure oscillations to decrease with time [16].

Theoretical and practical studies of transient fluid flow in the pipe have been of interest to many researchers in the last hundred years4]]. A number of researchers have also studied the phenomenon of water hammers according to the literature review mentioned as follows. Bayoumy and Papadopoulos [5] developed a method for analyzing steam hammers through a hot turbine power plant using commercial software from Caesar and PipeNet. The purpose of this research is to assist design engineers in the dynamic analysis of steam pipelines. Cao and Nistor [6] used a multi-step approach to investigate water hammers using the method of characteristics. They used the monolithic perspective and Gauss-Seidel algorithm and showed that the accuracy of problem solving is increased by using the integer values for the Courant number. In the next study [7], they used the asymmetric finite element method to analyze water hammer impact and the principle of mass and energy stability that are applied to determine the internal pressure distribution of the pipe and the temporal dependence of fluid energy using the finite element model. Chong et al. [8] proposed the Condensation Induced Water Hammer (CIWH) method for investigating the flow regime of condensed fluid under the influence of a water hammer in oscillating states and different pipe lengths. The criterion was to predict the flow regime from alternating to non-alternating state. Pham and Choi [9] simulated the effect of a steam hammer on steam pipes using the Computational Fluid Dynamics (CFD) method. The model includes energy and phase change equations and the Phyton algorithm is used to measure temperature and pressure changes results show that faster water flow reduces the impact of steam rams. Henclik [10] used a Shock Response Spectrum (SRS)-based numerical method to analyze water Hammer impact. Then the obtained data is compared with the experimental data to verify the results. The study showed an acceptable agreement of the results.

As can be concluded from previous research, the Method Of Characteristics (MOC) and the Finite-Element Method (FEM), or a combination of both, are the most common numerical methods used for solving the one-dimensional water Hammer impact. A different coupling approach consists of setting up an interaction between two different computer codes, one specific for the fluid and another for the structure. In each time step, the output information is transferred in both directions. There are contributions proposing methodologies to carry out this data transfer. However, the main challenge of this approach is the requirement of considerable computational effort, time consuming, and data transfer [3]. Furthermore, only a few authors investigated anchor and support behavior in the context of water hammer theory. In addition, understanding the governing equations that are in use in steam hammer research and practice and their limitations is essential for interpreting the results of the numerical models that are based on these equations, for judging the reliability of the data obtained from these models, and for minimizing misuse of water hammer models. Therefore, this research work aims to fill these gaps.

This research attempts to provide a simple yet, but an effective and approximate tool in terms of low cost, high-quality results, and low computational effort that can provide a bridge between hydro-mechanical data in the process of steam production. In addition, the Proposed model estimates the steam hammer force distributed in the multi-series pipeline by simplifying the real data model in the shortest possible time and lower cost than finite element or experimental models by entering the steam and piping parameters. The method of characteristics as a complement to the proposed theoretical model was applied and compared. The MOC method is a simple, accurate, effective numerical analysis method for analyzing one-dimensional transient currents with a constant pressure wave.

This paper is organized as follows, Section 2 introduces the proposed numerical MOC model. Section 3 presents the proposed theoretical model. Section 4 demonstrates the geometry of the physical model. Computational experiences are shown in section 5. Finally, section 6 outlines the findings and draws conclusions

2- Numerical MOC Model

A list of the symbols used in this research work and the according meanings is composed in Table 1. Joukowsky [11] who was the founder of the basic theoretical equation of water hammer states the amount of pressure changes as follows [4]

$$\Delta P = \pm \rho c \Delta V \tag{1}$$

where c is the wave speed, ρ is fluid density, and V is fluid velocity.

At fluid velocities much lower than the velocity of sound, the momentum continuity equation for fluid flow is given below [16]:

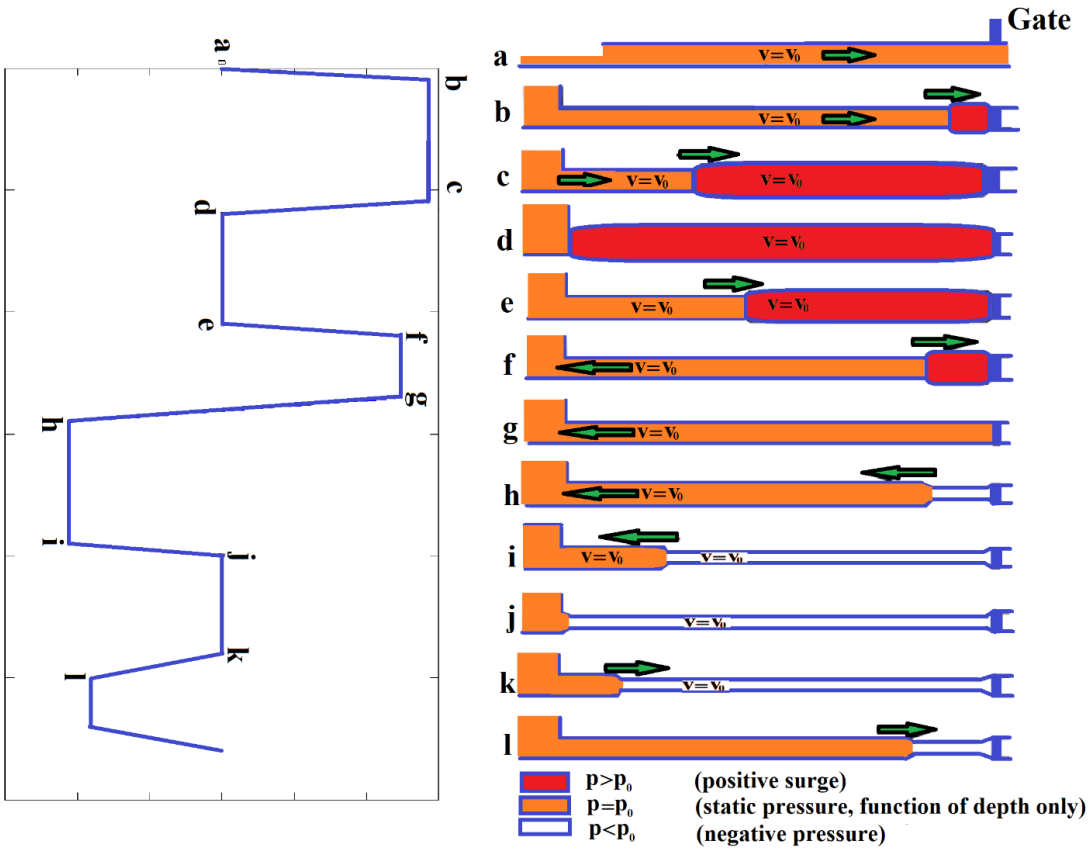

Fig. 1. Steam hammer transient

Table 1. list of Symbols and descriptions.

Symbol	Description	Symbol	Description
P	Fluid pressure	ω_n	Circular natural frequency
V	Fluid velocity	f_n	Natural frequency
T	Fluid temperature	τ'_n	Period of vibration
ρ	Fluid density	C_n	Damping coefficient
C	Wave speed	ζ	Critical damping ratio
f	Friction factor	D	Pipe diameter
r	Result of the global constant division of gases on molecular mass	L	Pipe length
π	Reduced pressure	E	Young modulus
τ	Reduced temperature	W	Unit weight of pipe length
F	Force	I	Inertia of the pipe cross section
t_{vct}	Valve close time	k	bulk modulus

$$\frac{\partial V}{\partial t}+\frac{1}{\rho}\cdot\frac{\partial P}{\partial x}+\frac{\tau_w\left(t\right)\pi D}{\rho A}=0$$
$$\frac{\partial P}{\partial t}+\rho c^2.\frac{\partial V}{\partial x}=0 \quad (2)$$

The water hammer classical equation neglects fluid compressibility. In this research, the equations for studying the transient fluid flow behavior along with the boundary conditions are analyzed and extracted. Accurate analysis of water hammer is completely dependent on accurate measurement of the friction of the pipe wall with the fluid. For this purpose, the Darcy-Weisbach equation is used according to the following equation [16].

$$\tau_\omega\left(t\right)=\left(\rho f\left(t\right)\left|V\left(t\right)\right|V\left(t\right)\right)/8 \quad (3)$$

where $f\left(t\right)$ is Darcy-Weisbach friction factor. Various unstable flow friction models have been considered for better adaptation to real results.

The transient flows continuity and momentum equation in a pipe can be described as [16]:

$$L_1=\frac{\partial V}{\partial t}+\frac{1}{\rho}\cdot\frac{\partial P}{\partial x}+\frac{f\left|V\right|V}{2D}=0$$
$$L_2=\frac{\partial P}{\partial t}+\rho c^2.\frac{\partial V}{\partial x}=0 \quad (4)$$

where distance (x) and time (t) are both independent variables but the pressure (P) and flow velocity (V) are two dependent variables. The other variables are assumed not to vary with time.

$L=L_1+\lambda L_2$, is linear combinatory of Eqs. (4). where λ is a linear coefficient. By repositioning the combination the following equation is obtained,

$$\left(\frac{\partial V}{\partial t}+\rho c^2\lambda.\frac{\partial V}{\partial x}\right)+\lambda\left(\frac{\partial P}{\partial t}+\frac{1}{\rho\lambda}\frac{\partial P}{\partial x}\right)+\frac{f\ |V\ |V}{2D}=0 \quad (5)$$

By total derivatives for the flow speed and pressure as follows, unknown coefficient λ is solved and Eq. (8) is derived:

$$\frac{dV}{dt}=\frac{\partial V}{\partial t}+\frac{\partial V}{\partial x}\frac{dx}{dt}$$
$$\frac{dP}{dt}=\frac{\partial P}{\partial t}+\frac{\partial P}{\partial x}\frac{dx}{dt} \quad (6)$$
$$\frac{1}{\rho\lambda}=\frac{dx}{dt}=\rho c^2\lambda$$

$$\lambda=\frac{\pm1}{\rho c} \quad (7)$$

$$\frac{dV}{dt}+\frac{1}{\rho c}\frac{dP}{dt}+\frac{f\left|V\right|V}{2D}=0$$
$$if\ \frac{dx}{dt}=c$$
$$\frac{dV}{dt}-\frac{1}{\rho c}\frac{dP}{dt}+\frac{f\left|V\right|V}{2D}=0 \quad (8)$$
$$if\ \frac{dx}{dt}=-c$$

In order to calculate the pressure and velocity of the flow, it is necessary to know the initial conditions in the first step. It should be noted that the friction losses in the above equation are nonlinear and are therefore considered constant flow velocities in engineering applications. If the results obtained are not acceptable, a shorter time period should be considered [16]:

$$\left(V_G-V_A\right)+\frac{1}{\rho c}\left(P_G-P_A\right)+\frac{f}{2D}\Delta tV_A\left|V_A\right|=0 \quad (9)$$

$$\left(V_G-V_B\right)-\frac{1}{\rho c}\left(P_G-P_B\right)+\frac{f}{2D}\Delta tV_B\left|V_B\right|=0 \quad (10)$$

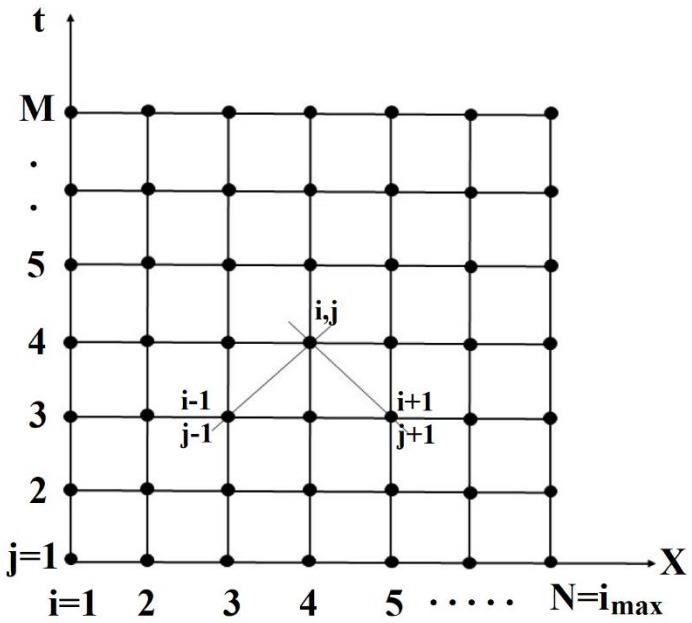

Fig. 2. Computational mesh/grid with index for MOC

$$\left(V_G - V_A\right) + \frac{1}{\rho c}\left(P_G - P_A\right) + \frac{fc}{2D}\Delta x V_A \left|V_A\right| = 0 \tag{11}$$

$$\left(V_G - V_B\right) - \frac{1}{\rho c}\left(P_G - P_B\right) + \frac{fc}{2D}\Delta x V_B \left|V_B\right| = 0 \tag{12}$$

The above equations are suitable for programming, and the index *i* and index *j* are the time variables shown in Fig. 2.

$$V_{i,j} - V_{i-1,j-1} + \frac{1}{\rho c}\left(P_{i,j} - P_{i-1,j-1}\right) + \frac{fc}{2D}\Delta x V_{i-1,j-1}\left|V_{i-1,j-1}\right| = 0 \tag{13}$$

$$V_{i,j} - V_{i+1,j-1} - \frac{1}{\rho c}\left(P_{i,j} - P_{i+1,j-1}\right) - \frac{fc}{2D}\Delta x V_{i+1,j-1}\left|V_{i+1,j-1}\right| = 0 \tag{14}$$

By rewriting Eq. (13) boundary conditions are organized at $x = 1$ and rewriting Eq. (14) the boundary conditions are organized at $x = 0$. Values for all nodes between boundary conditions are obtained by combining Eqs. (13) and (14) using Eqs. (15) and (16).

$$P_{i,j} = \frac{1}{2}\left(P_{i-1,j-1} + P_{i+1,j-1}\right) + \frac{\rho c}{2}\left(V_{i-1,j-1} - V_{i+1,j-1}\right) - \frac{\rho c}{2}\left(\frac{fc}{2D}\Delta x V_{i-1,j-1}\left|V_{i-1,j-1}\right| + \frac{fc}{2D}\Delta x V_{i+1,j-1}\left|V_{i+1,j-1}\right|\right) \tag{15}$$

$$V_{i,j} = \frac{1}{2}\frac{1}{\rho C}\left(P_{i-1,j-1} - P_{i+1,j-1}\right) + \frac{1}{2}\left(V_{i-1,j-1} + V_{i+1,j-1}\right) + \frac{1}{2}\left(\frac{fc}{2D}\Delta x V_{i+1,j-1}\left|V_{i+1,j-1}\right| + \frac{fc}{2D}\Delta x V_{i-1,j-1}\left|V_{i-1,j-1}\right|\right) \tag{16}$$

The flow equation for the boundary condition is:

$$P_0 = P_{i,j} + \frac{v_{i,j}^2 \rho}{2} \tag{17}$$

By rewriting Eq. (14):

$$P_{i,j} = P_{i+1,j-1} + \rho c \left(V_{i,j} - V_{i+1,j-1}\right) - \rho c \frac{fc}{2D} \Delta x V_{i+1,j-1} \left|V_{i+1,j-1}\right| \tag{18}$$

By inserting Eq. (18) into Eq. (17) and rewriting:

$$V_{i,j}^2 + 2cV_{i,j} - 2cV_{i+1,j-1} + \frac{2}{\rho}\left(P_{i+1,j-1} - P_0\right) - \frac{fc^2}{D} \Delta x V_{i+1,j-1} \left|V_{i+1,j-1}\right| = 0 \tag{19}$$

By solving Eq. (19):

$$V_{i,j} = -c + c \times \sqrt{1 + \frac{2V_{i+1,j-1}}{c} - \frac{2}{\rho c}\left(P_{i+1,j-1} - P_0\right) + \frac{f}{D} \Delta x V_{i+1,j-1} \left|V_{i+1,j-1}\right|} \tag{20}$$

Eq. (20) is applied for the boundary at $x = 0$.

The boundary condition near valve at discharge end of conduit:

$$P_{i,j} - P_{\text{end}} = K_L \frac{V_{i,j}^2 \rho}{2} \tag{21}$$

The loss coefficient (K_L), the flow velocity in the full conduit area A is rough estimated by:

$$K_L(t) \approx \left(\frac{A}{C_v a_v(t)} - 1\right)^2 \tag{22}$$

In this equation, C_v is the reduction coefficient equal to 1 for a smoothly curved entrance and $C_v a_v(t)$ is the vena-contracta area. The same approach is implemented for Eq. (13) [16]:

$$P_{i,j} = P_{i-1,j-1} - \rho c \left(V_{i,j} - V_{i-1,j-1}\right) - \rho c \frac{fc}{2D} \Delta x V_{i-1,j-1} \left|V_{i-1,j-1}\right| \tag{23}$$

$$V_{i,j}^2 + \frac{2c}{K_L(t)} V_{i,j} - \frac{2c}{K_L(t)} V_{i-1,j-1} - \frac{2}{\rho K_L(t)}\left(P_{i-1,j-1} - P_{\text{end}}\right) + \frac{fc^2}{DK_L(t)} \Delta x V_{i-1,j-1} \left|V_{i-1,j-1}\right| = 0 \tag{24}$$

By solving the above equations,

$$V_{i,j} = -\frac{c}{K_L(t)} + \frac{c}{K_L(t)} \times \sqrt{1 + \frac{2K_L(t)V_{i-1,j-1}}{c} - \frac{2K_L(t)}{\rho c^2}\left(P_{i+1,j-1} - P_0\right) - \frac{fK_L(t)}{D} \Delta x V_{i-1,j-1} \left|V_{i-1,j-1}\right|} \tag{25}$$

The proposed MOC method flowchart is presented in Fig. 3.

The IAWPS-IF 97 formula [13] is the basic equation for calculating the sound speed in steam. This equation is dimensionless and has two parts for calculating the free energy of Helmholtz $f(p,T)$ and the free energy of Gibbs $g(p,T)$. The basic equation for Gibbs' free energy is expressed in a dimensionless manner as follows:

$$\frac{g(p,T)}{rT} = \gamma(\pi,\tau) \tag{26}$$

In this equation, p is pressure, T is temperature, r is the result of the global constant division of gases on molecular mass, π is reduced pressure, and τ is reduced temperature. The function $\gamma(\pi,\tau)$ is defined by International Association for the Properties of Water and Steam (IAPWS) and the speed of sound is obtained from the following equation:

$$\mathrm{a}(\pi,\tau) = \sqrt{\frac{rT\left(\frac{\partial r}{\partial \pi}\right)^2 \tau^2 \frac{\partial^2 \gamma}{\partial \tau^2}}{\left(\frac{\partial r}{\partial \pi} - \tau \frac{\partial^2 \gamma}{\partial \pi \partial \tau}\right)^2 - \frac{\partial^2 \gamma}{\partial \pi^2} \tau^2 \frac{\partial^2 \gamma}{\partial \tau^2}}} \tag{27}$$

The visual solution of the above equation is shown in Fig. 4 [13].

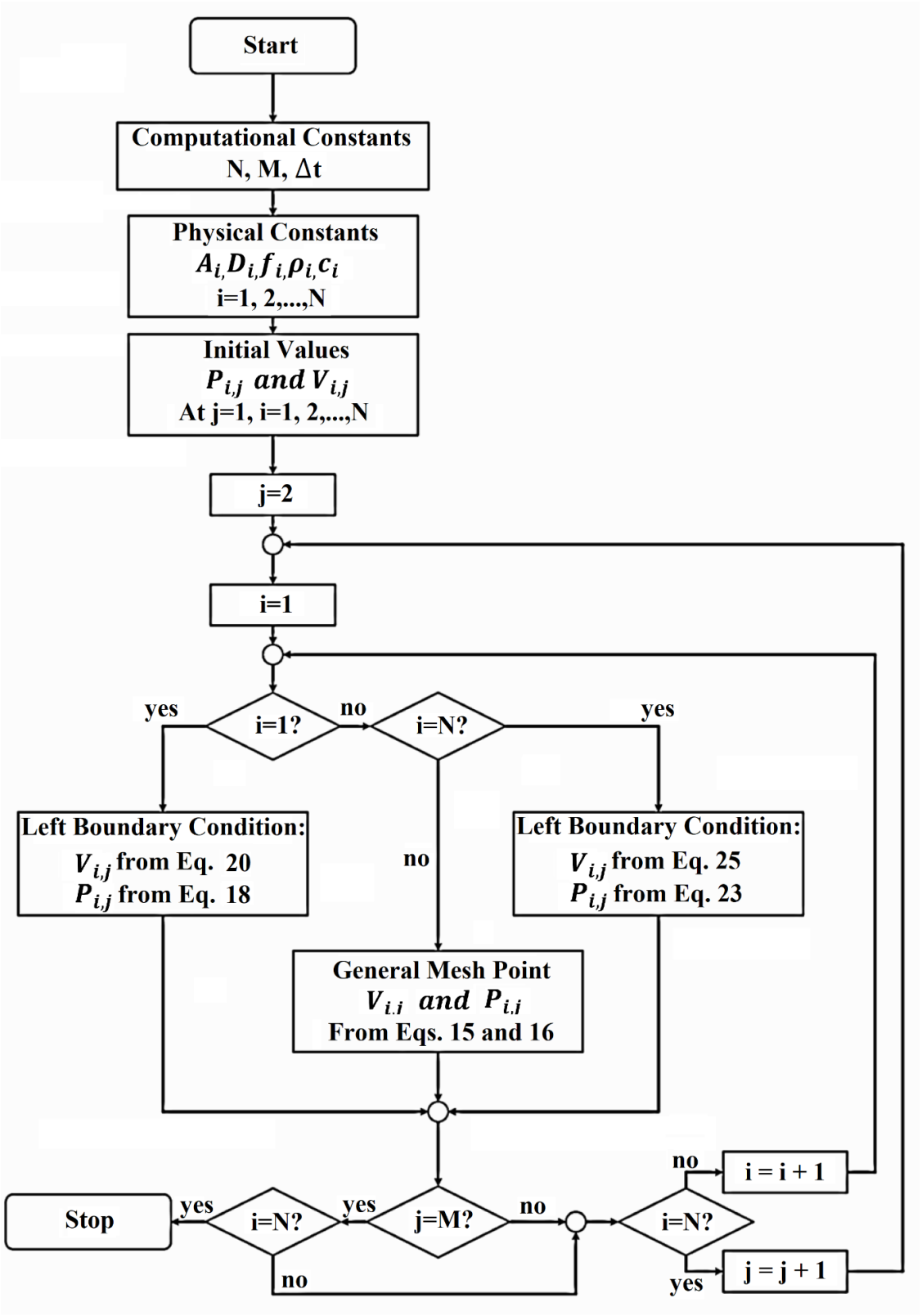

Fig. 3. Proposed MOC method flowchart

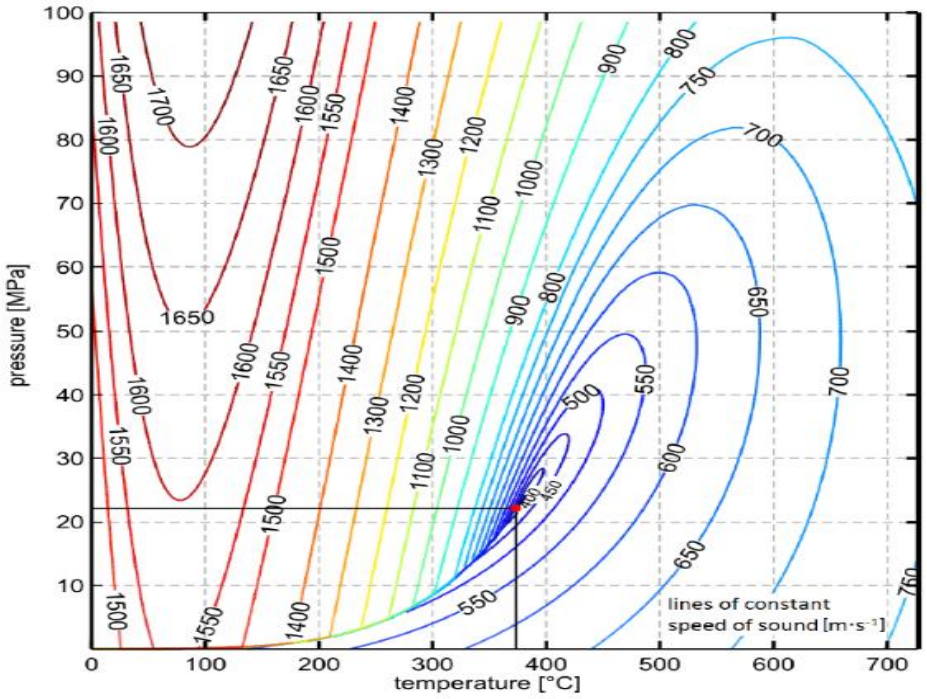

Fig. 4. Values for the speed of sound in steam and in steam in a P–T diagram [13].

3- Theoretical Model

To understand pipe failures due to steam hammer, the dynamics of generalized stresses require consideration. In this section, the equations governing the elastic stresses on the pipe are explained in successive steps. First, the equations for the temporal response of the induced vibration are expressed. Then, in the next step, the equations for temporal response to transient vibration related to impact excitation and sloping excitation are described. The dynamic response to an oscillating stimulus according to Newton's second law is as follows [17]:

$$m \cdot \frac{\mathrm{d}^2 x}{\mathrm{d}t^2} + 2 \cdot \zeta \cdot \omega_{\mathrm{n}} \cdot \frac{\mathrm{d}x}{\mathrm{d}t} + \omega_{\mathrm{n}}^2 \cdot x = F(t) \cdot g \tag{28}$$

Where

$$\zeta = \frac{c_n}{2 \cdot m \cdot \omega_n} = \frac{c_n}{c_{\text{critical}}} \tag{29}$$

$$\omega_{\mathrm{n}} = \sqrt{\frac{k^{'} \cdot g}{m}} = 2 \cdot \pi \cdot f_{\mathrm{n}} \tag{30}$$

$$\tau_{\mathrm{n}}^{'} = \frac{1}{f_{\mathrm{n}}} = \frac{2\pi}{\omega_{\mathrm{n}}} \tag{31}$$

ω_n is the circular natural frequency, f_n is the natural frequency, $\tau_n^{'}$ is the period of vibration, C_n is the damping coefficient, and ζ is the critical damping ratio. Damping and frequency effects can be described using a free vibration equation [17]. Accurate damping coefficient based on Hadjian's [15] experimental data is obtained. This data is from tests performed on the steam pipes of the power plant is attained. Statistical data have shown that welding, insulation, the liquid inside the pipe as well as various loads such as valves affect the damping coefficient. Hajian's equation gives a more accurate estimate than the code ASCE-43:

$$\zeta = 0,0053 + 0,0024 \cdot D + 0,0166 \cdot R + 0,009 \cdot FM - 0,0019 \cdot LD \tag{32}$$

where D is the nominal pipe diameter, $R = 0$ if yielding occurs, $R = 1$ if there is no yielding, $FM = 1$ for the first mode, $FM = 0$ for all other modes, $LD = 1$ if there are equipment or loads on the pipe, and $LD = 0$ for no loads on the pipe. The general solution for the response to a suddenly applied force is then expressed as [17]

$$\frac{X(T),K'}{F} = \left(1-\frac{e^{-\zeta\cdot\omega\cdot t}}{\sqrt{1-\zeta^2}}\cdot\cos\left(\left(t\cdot\omega\cdot\sqrt{1-\zeta^2}\right)-\left(\frac{\zeta}{\sqrt{1-\zeta^2}}\right)\right)\right) = S(t,\omega,\zeta) \quad (33)$$

By the way, the general solution for the response to a ramp applied force with t_1 duration is stated by [17]:

$$x = \frac{F}{k'}\cdot\left(1-\left(\frac{\zeta}{\sqrt{1-\zeta^2}}\right)-\frac{e^{-\zeta\omega t}}{\sqrt{1-\zeta^2}}\cdot \cos\left(\left((t-t_1)\cdot\omega\cdot\sqrt{1-\zeta^2}\right)-\left(\frac{\zeta}{\sqrt{1-\zeta^2}}\right)\right)\right)\times \left(1-\left(\frac{\zeta}{\sqrt{1-\zeta^2}}\right)-\frac{e^{-\zeta\cdot\omega t}}{\sqrt{1-\zeta^2}}\cdot \cos\left(\left(t\cdot\omega\cdot\sqrt{1-\zeta^2}\right)-\left(\frac{\zeta}{\sqrt{1-\zeta^2}}\right)\right)\right) \quad (34)$$

The dynamic magnification factor for a step response is initially stated in terms of the Percent Overshoot (P.O.). The structural damping coefficient ratio can be calculated as follows [17]:

$$\mathrm{DMF} = 1+\mathrm{P.O.} = \left(1+e^{\left[\frac{-\zeta\cdot\pi}{\sqrt{1-\zeta^2}}\right]}\right) \quad (35)$$

The dynamic stress expression prepares a reduced expression for the response of simple systems, such as conduit, bars, or pipe supports. A common expression for the DMF of a single Degree of Freedom (DOF) structure is [17]

$$V''(t) = \frac{x''(t)\cdot k''}{F} \quad (36)$$

Where $V''(t) = S(t)$ step , $I(t)$ impulse , $R(t)$ ramp , or $C(t)$ harmonic responses may be derived as required from Harris and Piersol [14]. The step response is an important dynamic stress equation for this work, so that the step response draws suddenly applied constant loads to conduits that are characteristic of some steam hammer loads to outcome [17]

$$F(t) = F'\cdot\left(1-\frac{e^{-\zeta\cdot\omega\cdot t}}{\sqrt{1-\zeta^2}}\cdot\cos\left(t\cdot\omega\cdot\sqrt{1-\zeta^2}\right)-\mathrm{atan}\left(\frac{\zeta}{\sqrt{1-\zeta^2}}\right)\right) \quad (37)$$

If coordinate axes are neglected to simplify discourses and explanations but Triple axial vibrations need attention. For instance, the step vibration response of Eq. (36) is rewritten as [17]

$$F_j(t) = F_j'\cdot\left(1-\frac{e^{-\zeta_j.\omega_j\cdot t}}{\sqrt{1-\zeta_j^2}}\cdot\cos\left(t\cdot\omega_j\cdot\sqrt{1-\zeta_j^2}\right)-\mathrm{atan}\left(\frac{\zeta_j}{\sqrt{1-\zeta_j^2}}\right)\right) \quad (38)$$

Where j describes axial directions, and $j = x, y, z$. The fact is that vibrations in a structure are coupled vibrations. The vibrations need to be uncoupled to implement the dynamic stress equation. Otherwise, matrix techniques must be employed to analyze vibrations [17].

In this stage, we will consider the one-dimensional wave propagation equation via the method of standing variables including one that is a Fourier series. The wave speed equation is applicable to waves in gases, fluids, or solids. In fact, the wave speed equation can be used to derive vibration equations, which is appropriate since shock waves on structures induce vibrations. The general form of the wave speed equation in elastic materials is frequently referred to as the D'Alembert equation and is expressed as

$$\frac{\partial^2 H(x,t)}{\partial x^2} = \frac{1}{c^2}\frac{\partial^2 H(x,t)}{\partial t^2} \quad (39)$$

Furthermore, we will then consider traveling wave solutions of this wave equation, including one that is a Fourier series. A common sine wave with wavelength $\lambda = 2\pi/k$, amplitude B , traveling with speed c is

$$H(x,t) = B\sin(k(x-ct)) \quad (40)$$

This formula gives a sinusoidal curve and other shapes can be made from an added of sines and cosines. The square wave, defined by

$$H(x,t=0)=\begin{cases}+1 & 0<x<L/2\\ -1 & L/2<x<L\end{cases} \tag{41}$$

This can be explained by the sum of sine waves

$$H(x,t=0)=\sum_{n=2,6,10,14,\ldots}\frac{8}{n\pi}\sin\left(\frac{n\pi x}{L}\right) \tag{42}$$

This special square wave only contains all 4th term, the n = 3 to 9 terms are zero except $n=6$ is non-zero and so forth. Initiate with this square wave moving with speed c at $t=0$ is acquired by reducing ct from x in the argument of the sine waves, i.e.,

$$H(x,t)=\sum_{n=2,6,10,14,\ldots}\frac{8}{n\pi}\sin\left(\frac{n\pi(x-ct)}{L}\right) \tag{43}$$

The first few terms are

$$\begin{aligned}H(x,t)=&\frac{4}{\pi}\sin\left(\frac{2\pi(x-ct)}{L}\right)+\\ &\frac{4}{3\pi}\sin\left(\frac{6\pi(x-ct)}{L}\right)+\\ &\frac{4}{5\pi}\sin\left(\frac{10\pi(x-ct)}{L}\right)+\cdots\end{aligned} \tag{44}$$

The net shaking force at each piping leg is taken as the difference in the pressure existing at both ends of the pipe leg under consideration. The maximum shaking force, $F_{\max}$, is determined by the length of the leg. If the length of the leg is greater than the sonic velocity times the effective valve close time, the maximum shaking force is the same as the maximum surge force, F_t. If the leg length is shorter than the sonic velocity multiplied by the valve closing time, the maximum shaking force is determined by direct proportion as:

$$F_{\max}=F_t\frac{l_{ij}}{t_{vct}c}\quad\left(\text{for } l_{ij}<t_{vct}c\right) \tag{45}$$

where l_{ij} is the length of the pipe leg located between point i and point j. Then induced force by steam hammer can be calculated by:

$$\begin{aligned}F(x,t)=&A\times\rho\times V\times\left[\frac{L}{t_{vct}}-\left\langle\frac{L}{t_{vct}}-1\right\rangle\right]\times\\ &\left\{\sqrt{\frac{rT\left(\frac{\partial\gamma}{\partial\pi}\right)^2\tau^2\frac{\partial^2Y}{\partial\tau^2}}{\left(\frac{\partial Y}{\partial\pi}-\tau\frac{\partial^2Y}{\partial\pi\partial\tau}\right)^2-\frac{\partial^2Y}{\partial\pi^2}\tau^2\frac{\partial^2Y}{\partial\tau^2}}}\times\left(1+e^{\left[\frac{-\zeta\cdot\pi}{\sqrt{1-\zeta^2}}\right]}\right)\times\right.\\ &\left.\left[\begin{array}{l}\frac{4}{\pi}\sin\left(\frac{2\pi(x-ct)}{L}\right)+\frac{4}{3\pi}\sin\left(\frac{6\pi(x-ct)}{L}\right)+\\ \frac{4}{5\pi}\sin\left(\frac{10\pi(x-ct)}{L}\right)+\cdots\end{array}\right]\right\}\end{aligned} \tag{46}$$

4- Proposed Pipeline Model

For analysis of steam hammer in multi-series steam turbine pipeline using proposed theoretical model and method of characteristics, the piping system shown in Fig. 5 has been used.

The specifications of this model are as follows:

-Pipe Material: Low Carbon Steel

-Fluid inside the pipe: hot steam

-Fluid temperature: 750 °F

-Fluid pressure: 500 PSIA

-Insulating pipe: C.S. (Special type of glass fiber reinforcement composite)

-Reference Standard: ASME B31.1

-Permissible ambient temperature stress of pipe steel: 17,000 PSIA

-Permissible working temperature stress of pipe steel: 10950 PSIA

-Fluid speed inside the pipe: 45 ft/s

Table 2 shows the list of components of the Piping System as shown in Fig. 5**.** The proposed piping system layout is based on the actual steam production line from the boiler to the steam turbine. The model is designed based on the code ASME B31.1. This model has four series, each series is divided into a number of segments. Each segment is also located on rigid supports. In order to increase the flexibility of leg #1, fixed support is omitted at the end of leg #1. At the end of leg #1, a snubber (shock absorber) is used to absorb the shock caused by the steam hammer. One of the practical goals of this research is to estimate the force exerted on this shock absorber. The length of each segment in order to increase the computational accuracy should be selected based on preventing segments' rigidity and geometric shape loss due to excessive bending. For this purpose, according to the code, ASME B31.1, maximum length of each segment is determined by:

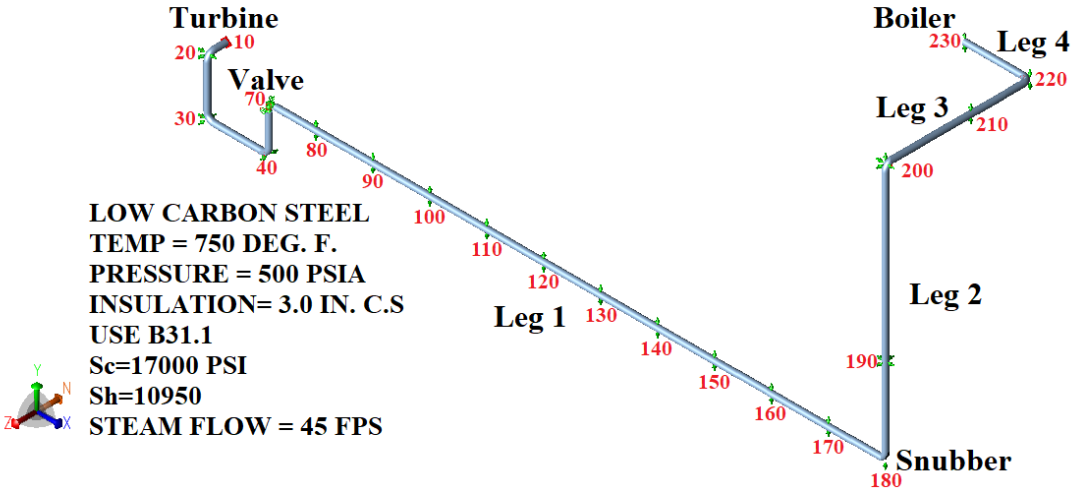

Fig. 5. The proposed Multi-segment pipeline.

Table 2. List of Fig. 5 piping system elements

From Node	To Node	Length ft. OD 12.75 in Wall THK 0.688 in
10	20	4
20	30	12
30	40	13
40	50	8
50	60	1.42
60	70	1.42
70	80	8.5
80	90	12
90	100	12
100	110	12
110	120	12
120	130	12
130	140	12
140	150	12
150	160	12
160	170	12
170	180	12
180	190	18
190	200	36
200	210	18
210	220	12.5
220	230	13.75

Leg #1
Leg #2
Leg #3
Leg #4

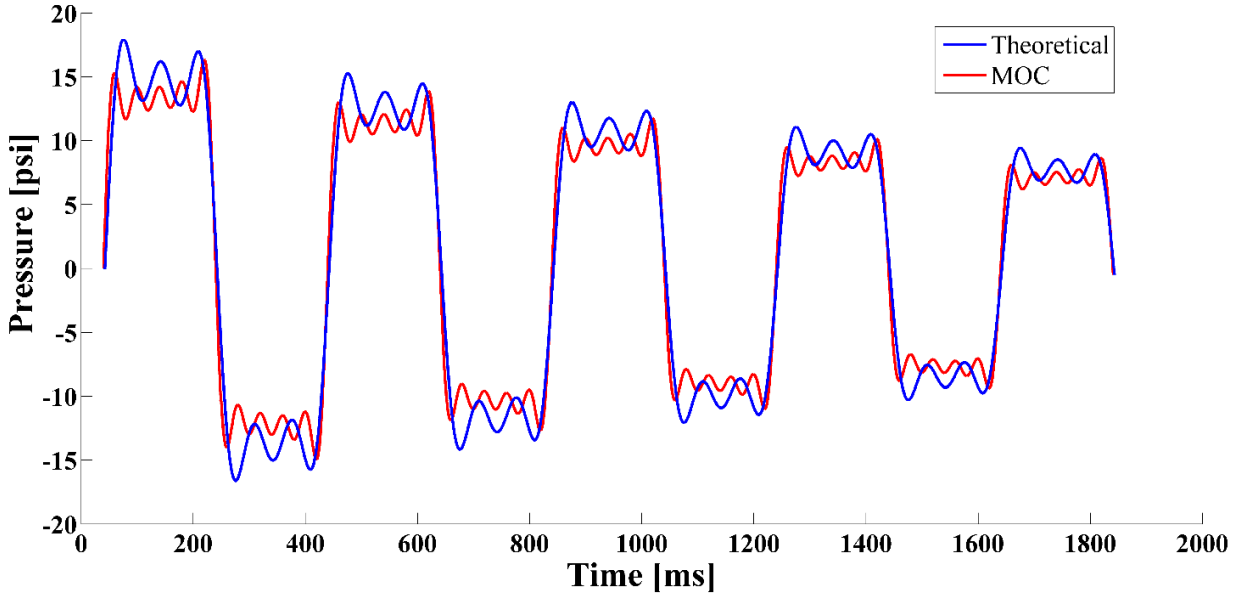

Fig. 1. The compared Pressure wave propagation - time by different computational tools- pipeline #1.

$$L = \sqrt[4]{\frac{128EI\Delta}{\mathrm{w}}} \tag{47}$$

Where E , I , W and Δ are the young modulus, the inertia of the pipe cross section, W unit weight of pipe length and permissible pipe mid-deflection respectively. According to code ASME B31.1,, the maximum allowed mid-deflection is less than 0.1 inches.

5- Results and Discussion

This study attempts to calculate accurately the dynamic force of the steam hammer caused by the fluid transient of the sudden closure of the flow control valve. The closing time of the pneumatic valve is considered 10 milliseconds. For this purpose, the proposed MOC numerical model programmed in MATLAB software and proposed piping layout were implemented. The obtained results are compared with the proposed theoretical model. At first, the compared Pressure wave propagation by different computational tools for pipeline #1 is drawn as shown in Fig. 6. Pressure wave (for an instantaneous valve closure) calculated with Joukowsky's fundamental equation of steam hammer. If the steam hammer only affects the steam, the wave speed would be the speed of sound in steam. However, the elastic pipe expands due to the increased pressure, sending out a wave in the structure as well. The structural wave is approximately four times faster than the one in the fluid. This causes an interaction between the fluid and the structure, resulting in a slower wave speed than the sonic speed in steam.

Flowmaster software was also used for further validation. Flowmaster is an advanced Computer-Aided Engineering (CAE)/CFD Virtual Systems Modelling tool that enables engineers to model the most challenging transient hydraulic problems in complex systems. Flowmaster's Transient module provides the capability to model time-dependent events in a real flow situation. To enable Transient modeling additional data is required for certain components. The wave speed suggested by Flowmaster is calculated from:

$$C = \sqrt{\frac{1}{\rho\left(\frac{1}{k} + \frac{D\Phi}{tE}\right)}} \tag{48}$$

where $\rho =$ liquid density, $k =$ bulk modulus of liquid, $D =$ pipe internal diameter, $t =$ pipe thickness, $E =$ Young's Modulus of pipe material, and ϕ is pipe restraint factor. Flowmaster provides the rigid and elastic pipe models for simulating pipes in a Transient simulation. Elastic pipe models the full elastic behavior of a pipe containing a liquid in motion (or which can be set in motion). Therefore, in this research work, the elastic model is proposed and the method of characteristics is used. Therefore, it is required to define a distance-time grid for all elastic pipes in the network. In order to simulate in Flowmaster, pipeline layout implemented, wave speed and valve data input and output data established. The results for the first cycle are shown in Fig. 7 and 8. Fig. 7 shows the calculations for series number one and Fig. 8 shows the same parameters for series number two. As shown in the figures, the results of all three methods are well matched by a 7% difference. The waveform in series two has changed compared to series one. In this series, the difference between the theoretical method and the other two methods in terms of form and amplitude increased, but still shows an acceptable

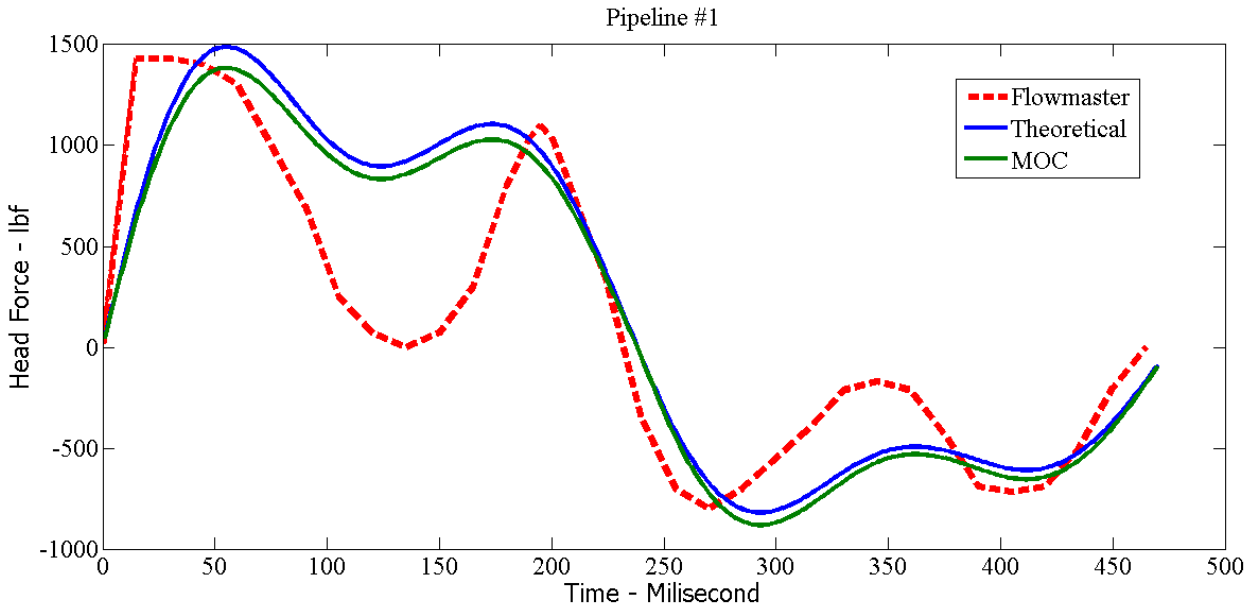

Fig. 7. The compared head force - time on different computational tools- pipeline #1.

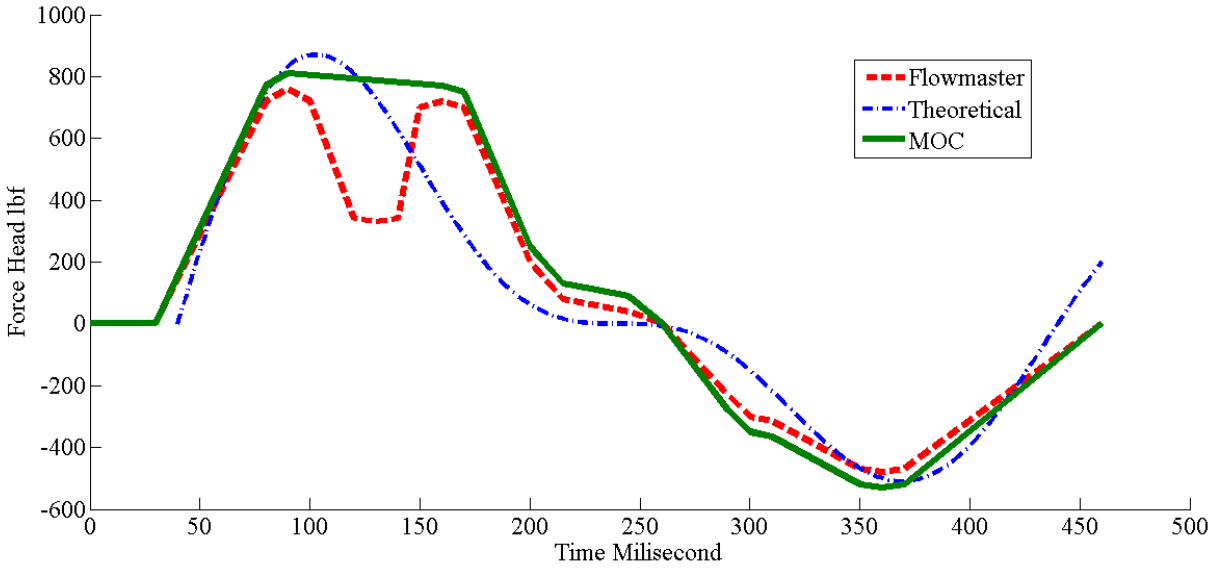

Fig. 8. The compared head force - time on different computational tools- pipeline #2.

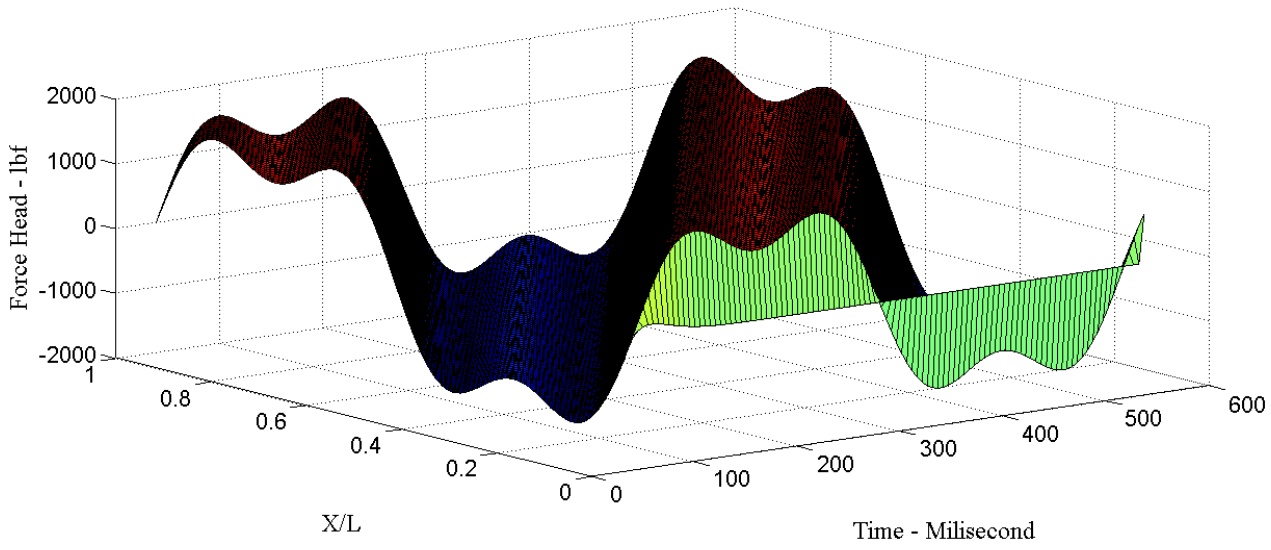

Fig. 9. The behavior of proposed theoretical steam hammer wave propagation in terms of time and longitudinal distance.

agreement by a 9% difference. Another important point is that the theoretical method has a pre-phase compared to other methods. In other words, it peaks faster and decreases faster. This seems to be due to the lack of friction consideration in the theoretical model.

For keen readers, the behavior of the theoretical model set against time and place simultaneously may be interesting. For this purpose, the pressure head diagram in terms of time and relative position along the pipe is presented in Fig. 9**.**

The behavior of a wave function based on both time and distance as can be seen from Fig. 8, is sinusoidal. The frequency in terms of time is much higher than the frequency in terms of distance. It also changes shape as the wave travels over the distance. This is confirmed by the difference in the waveform in Fig. 8 compared to Fig. 7.

From another perspective, one of the objectives of this research is to calculate the dynamic inductive force from the steam hammer to the shock absorber. This shock absorber is located at the end of series one. The force applied to this shock absorber is obtained from Eq. (46), which Equals 2731 lbf. In order to validate the mentioned force, the pipeline model has been simulated in CAESAR software and the obtained force has had only a 4% error from the theoretical model.

6- Conclusion

The aim of this study is to study the effect of a steam hammer on a steam turbine multi-series line and calculation the force on the shock absorber at the end of the main pipeline by low computational effort and less costly setup. The goals of this research are:

- Accurate calculation of wave speed propagation is constructed.
- A simple yet, but effective and approximate tool that can provide a bridge between hydro-mechanical data in the process of steam production is provided.
- The steam hammer force is distributed in the piping by simplifying the real data model quickly estimated.
- proposed theoretical model overcomes the drawback of the method of characteristics in terms of computational effort and experimental methods in terms of costly and labor-intensive setup.
- For more reassurance, results are compared with the MOC method and Flowmaster package. Results show good conformity in series one by %7 difference and acceptable agreement in series two by 9% difference respectively with the proposed theoretical model.
- Moreover, In order to validate the obtained steam hammer force, the pipeline model was simulated in CAESAR software and the result has only a 4% error from the theoretical model.

References

[1] J. Korteweg, Ueber die Fortpflanzungsgeschwindigkeit des Schalles in elastischen Röhren (On the transmission of sound by fluids enclosed in tubes with elastic walls); Ann. der Physik and Chemie, (1878) 525-542.

[2] H.L.F. Helmholtz, von, Bericht über die theoretische Akustik betreffenden Arbeiten vom Jahre, In: Die Fortschritte der Physik, Berlin, 4 (1848)101-118.

[3] D. Ferras, P.A. Manso, A.J. Schleiss, D.I.C. Covas, One-Dimensional Fluid–Structure Interaction Models in Pressurized Fluid-Filled Pipes: A Review, Applied Sciences, 8(10) (2018) 1844.

[4] M.S. Ghidaoui, M. Zhao, D.A. McInnis, D.H. Axworthy,

A Review of Water Hammer Theory and Practice, Applied Mechanics Reviews, 58(1) (2005) 49-76.

[5] A.H. Bayoumy, A. Papadopoulos, Time History Steam Hammer Analysis for Critical Hot Lines in Thermal Power Plants, ASME 2014 International Mechanical Engineering Congress and Exposition, (2014).

[6] H. Cao, M. Mohareb, I. Nistor, Partitioned water hammer modeling using the block Gaus“ Seidel algorithm, Journal of Fluids and Structures, 103 (2021) 103260.

[7] H. Cao, M. Mohareb, I. Nistor, Finite element for the dynamic analysis of pipes subjected to water hammer, Journal of Fluids and Structures, 93 (2020) 102845.

[8] D. Chong, W. Liu, Q. Zhao, J., Yan , T. Hibiki, Oscillation characteristics of periodic condensation induced water hammer with steam discharged through a horizontal pipe. International Journal of Heat and Mass Transfer, 173(2021) 121265.

[9] T. Q. D. Pham, S. Choi, Numerical analysis of direct contact condensation-induced water hammering effect using Open FOAM in realistic steam pipes. International Journal of Heat and Mass Transfer, 171(2021) 121099.

[10] S. Henclik, Application of the shock response spectrum method to severity assessment of water hammer loads. Mechanical Systems and Signal Processing, 157(2021) 107649.

[11] N. E. Joukowski, On the hydraulic hammer in water supply pipes. ‘‘Memoirs of the Imperial Academy Society of St. Petersburg,’’ 9(5) (Russian translated by O Simin 1904), Proc. Amer. Water Works Assoc, 24 (1898) 341–424.

[12] M.H. Chaudhry, Applied hydraulic transients. , 3rd ed. , Springer New York, (2014).

[13] IAPWS, Revised release on the IAPWS industrial formulation 1997 for the thermodynamic properties of water and steam, IAPWS R7-97(2012), The International Association for the Properties of Water and Steam, Switzerland, (2007).

[14] C. M. Harris, A. G. Piersol, Shock and Vibration Handbook, 6rd ed. ,McGraw Hill, New York, (2002).

[15] A. T., Hadjian, H. T. Tang, Identification of the Significant Parameters Affecting Damping in Piping Systems, 1rd ed. , American Society of Mechanical Engineers, New York, (1986).

[16] J. Carlson, Water Hammer Phenomenon Analysis using the Method of Characteristics and Direct Measurements using a “stripped” Electromagnetic Flow Meter, Published Thesis, Division of Nuclear Reactor Technology, Department of Physics, Royal Institute of Technology, Stockholm, Sweden, (2016).

[17] R. A. Leishear, Fluid Mechanics, Water Hammer, Dynamic Stresses, and Piping Design, 1rd ed., Savannah River National Laboratory, ASME, 3 Park Avenue, New York, (2012).

HOW TO CITE THIS ARTICLE

H. Nouri, Development of Theoretical Model to calculate Steam Hammer Force on Shock Absorber in Multi Series Pipeline , AUT J. Mech Eng., 6(3) (2022) 315-330.

DOI: 10.22060/ajme.2022.20897.6023